Code:2-117

Wave Passage and Incoherency Effects on Nonlinear Response of High Arch Dams

M.Akbari [1] , R. Naderi [2]

1-Ph.D. Student, Shahrood University ,masomeh.akbari@gmail.com
2-Assistant Professor , Shahrood University

ABSTRACT

In the present paper, effects of incoherency and wave-passage on nonlinear responses of concrete arch dams were investigated. A double curvature arch dam was selected as numerical example. Reservoir was modeled as a compressible material and foundation was modeled as a mass-less medium. Ground motion time-histories were artificially generated using Monte Carlo simulation approach. Four different FE models were considered including; Uniform excitation; Incoherence effect; Wave passage effect and; finally both incoherence and wave passage effects. It was revealed that modeling multiple-supports excitation could have significant effects on the structural response of the dam by inducing pseudo-static effect. Also, it was concluded that coherency effect overshadow wave passage effect and results obtained from non-uniform exciting of FEM including wave passage effect is close to the results of the FE model exited uniformly.

Keywords: Concrete Arch Dam, Incoherency, Nonlinear analysis, Wave passage

1. INTRODUCTION

Past researches have shown that seismic ground motion can vary significantly over distances comparable to the length of the long-span structures. As a result, such structures are subjected to ground motions at their supports that can differ considerably in amplitude, phase, as well as frequency content. In some cases, these differential motions can induce additional internal forces in the structure when compared to the case of identical support ground motion. This in turn might have a potentially detrimental effect on the safety of large structures during a severe earthquake event. Spatially variation earthquake ground motion (SVEGM) can be mainly attributed to the following three mechanisms: wave passage effect, incoherence effect and local soil effect. Harichandran et al. [1] considered both the effects of wave passage and incoherence in their model to estimate the response of single span beam using a random vibration approach. They concluded that by considering only the wave passage effect the beam response is underestimated and that the assumption of identical support ground motion was overly conservative for the case of single span beam. Zerva [2] investigated the effects of both loss of coherence and phase difference between the motions at the supports and separated the contribution of the different coherency models to the quasi-static and dynamic response of linear generic models of lifelines [2,3,4,5]. He concluded that the loss of coherence effect overshadows the wave passage effect and in fact, the wave propagation effect may be neglected at sites where ground motion is expected to be incoherent. As the velocity of wave propagation increases, the contribution of the quasi-static term drops and that of the dynamic term increases.

Responses of dams to SVEGM have been studied by Bayraktar [6], Maeso et al. [7], Chen and Harichandran [8]. Mirzabozorg et al. [9,10] investigated the effects of non-uniform excitation due to spatially variation of seismic waves under the reservoir bottom on linear and nonlinear responses of arch dams. It was observed that the non-uniform excitation decreases the crest displacements in the stream directions in comparison with the cases exciting the system uniformly. In addition, it was found that the results obtained from the model with uniform excitation are too conservative. In nonlinear analyses it was found that there is no cracked Gaussian point when non-uniform excitation is applied under the reservoir. Bayraktar et al. [11,12] analyzed the effect of wave propagation on the response of Sariyar concrete gravity dam. They reported that horizontal, vertical and shear stresses on the foundation generally increase with decreasing the propagation velocity and at a cross section close to the base of the dam, horizontal stresses also increase with decreasing the velocity but vertical and shear stresses do not exhibit a consistent pattern. Alves and Hall [13,14] analyzed the effect of SVEGM on the nonlinear response of Pacoima dam using available seismic data. Results showed that for uniform excitations stresses and joint opening were largest in the center part of the dam away from the abutments. Also, cracks formed mostly in the central part. The stresses along the abutments and in the center on the downstream face of the dam were dominated by the pseudo-static response, whereas those near the center section of the crest by the dynamic contribution. Similarly, joint opening was caused by the pseudo-static effects along the abutments but by the dynamic contribution at the central part of the dam. Recently, Chopra and Wang [15] considered the response of two arch dams to spatially varying ground motions recorded during earthquake by developed linear analysis procedure, which includes dam-water-foundation rock interactions effects. They concluded that the influence of SVEGM for the same dam could differ from one earthquake to the next, depending on the epicenter location and the focal depth of the earthquake relative to the dam site.

In the present paper, effects of incoherence and wave-passage on nonlinear responses of concrete arch dams are investigated by developing a computer code utilizing Monte Carlo approach which is able to consider incoherence and wave passage effects for generation of artificial earthquake ground motions. Four different models were considered in generation of ground motions, which are; uniform ground motion; ground motion including incoherence effect; ground motion including wave passage effect; and ground motion including both incoherence and wave passage effects. Finite element model of a high arch dam was prepared considering all required features for nonlinear seismic analysis of these kinds of structures.

2. GENERATION OF SVEGM

One of the most important parts of the Monte Carlo simulation methodology is generation of sample functions of stochastic processes, fields or waves involved in the problem. The generated sample functions must accurately describe the probabilistic characteristics of the corresponding stochastic processes, fields or waves that may be either stationary or non-stationary, homogeneous or non-homogeneous, one dimensional or multi-dimensional, uni-variate or multi-variate, Gaussian or non-Gaussian.

2.1. m-VARIATE NON-STATIONARY STOCHASTIC GROUND MOTION PROCESSES

Following the spectral-representation methodology [16] consider the 1D-mV (one-dimensional, m-variate) non-stationary ground motion stochastic vector process [17], whose components $f_j^0(t)$; $j = 1, 2, ..., m$ have zero mean, i.e.:

$$\varepsilon\left[f_j^0(t)\right]=0\ ,\ j=1,2,...,m \qquad (1)$$

Cross-correlation matrix is given by:

$$R_f{}^0(t,t+\tau)=\begin{bmatrix} R_{11}^0(t,t+\tau) & R_{12}^0(t,t+\tau) & \cdots & R_{1m}^0(t,t+\tau) \\ R_{21}^0(t,t+\tau) & R_{22}^0(t,t+\tau) & \cdots & R_{2n}^0(t,t+\tau) \\ \vdots & \vdots & \ddots & \vdots \\ R_{m1}^0(t,t+\tau) & R_{m2}^0(t,t+\tau) & \cdots & R_{mm}^0(t,t+\tau) \end{bmatrix}_{m\times m} \qquad (2)$$

and corresponding cross-spectral density matrix with evolutionary power spectrum is given by:

$$S^0(\omega,t)=\begin{bmatrix} S_{11}^0(\omega,t) & S_{12}^0(\omega,t) & ... & S_{1m}^0(\omega,t) \\ S_{21}^0(\omega,t) & S_{22}^0(\omega,t) & ... & S_{2m}^0(\omega,t) \\ \vdots & \vdots & \ddots & \vdots \\ S_{m1}^0(\omega,t) & S_{m2}^0(\omega,t) & ... & S_{mm}^0(\omega,t) \end{bmatrix}_{m\times m} \qquad (3)$$

Due to the non-stationarity of the vector process, the cross-correlation matrix is a function of both time "t" and time lag "τ", while the cross-spectral density matrix is a function of both frequency "ω" and time "t". It has to be emphasized that under the hypothesis of fully non-stationary processes (non-stationary processes with amplitude and frequency modulation), the cross-spectral density matrix is a non-separable function of frequency "ω" and time "t". Specifically for the case of earthquake ground motion, the elements of the cross-spectral density matrix with evolutionary power can be expressed in the following special form:

$$\begin{aligned} &S_{jj}^0(\omega,t)=|A_j(\omega,t)|^2\ S_j(\omega)\ \ ;\ \ j=1,2,\ldots,m \\ &S_{jk}^0(\omega,t)=A_j(\omega,t)A_k(\omega,t)\sqrt{S_j(\omega)S_k(\omega)}\Gamma_{jk}(\omega)\ \ ;\ \ j\neq k\ \ \&\ j,k=1,2,\ldots,m \end{aligned} \qquad (4)$$

where, $A_j(\omega,t)$ and $S_j(\omega)\ ;\ j=1,2,\ldots,m$ are the (non-separable) modulating function and the (stationary) power spectral density function of component $f_j^0(t)\ ;\ j=1,2,...,m$ respectively, and $\Gamma_{jk}(\omega)\ ;\ j\neq k\ \&\ j,k=1,2,\ldots,m$ is the complex coherence function between $f_j^0(t)$ and $f_k^0(t)$. The cross spectral density matrix $S_j^0(\omega,t)$ is Hermitian and satisfies the following properties [16]:

$$S_{jj}^0(\omega,t)=S_{jj}^0(\text{-}\omega,t)\ ;\ \ j=1,2,\ldots,m\ \forall t \qquad (5)$$

with the off-diagonal elements being generally complex functions of "ω" satisfying:

$$S_{jk}^0(\omega,t)=S_{jk}^{0*}(\text{-}\omega,t)\ \ ;\ \ j=1,2,\ldots,m;\ \ j\neq k\ \forall t \qquad (6)$$

and,

$$S_{jk}^0(\omega,t)=S_{kj}^{0*}(\text{-}\omega,t)\ ;\ \ j=1,2,\ldots,m;\ \ j\neq k\ \forall t \qquad (7)$$

where, the asterisk denotes the complex conjugate. Moreover, the elements of the cross-correlation matrix are related to the corresponding elements of the cross-spectral density matrix through the following transformations.

$$R_{jj}^{0}(t,t+\tau)=\int_{-\infty}^{+\infty}A_j(\omega,t)A_j(\omega,t+\tau)S_j(\omega)e^{i\omega\tau}d\omega\;;\; j=1,2,\ldots,m \qquad (8)$$

$$R_{jk}^{0}(t,t+\tau)=\int_{-\infty}^{+\infty}A_j(\omega,t)A_k(\omega,t+\tau)\sqrt{S_j(\omega)S_k(\omega)}e^{i\omega\tau}d\omega\;;\; j,k=1,2,\ldots,m\;;\; j\neq k \qquad (9)$$

For the special case of uniformly modulated non-stationary stochastic vector process, the modulating functions are independent of the frequency, that is:

$$A_j(\omega,t)=A_j(t)\quad,\; j=1,2,\ldots,m \qquad (10)$$

In this special case, Eqs 8 and 9 are reduced to:

$$R_{jj}^{0}(t,t+\tau)=A_j(t)A_j(t+\tau)\int_{-\infty}^{+\infty}S_j(\omega)e^{i\omega\tau}d\omega\;;\; j=1,2,\ldots,m \qquad (11)$$

$$R_{jk}^{0}(t,t+\tau)=A_j(t)A_k(t+\tau)\int_{-\infty}^{+\infty}\sqrt{S_j(\omega)S_k(\omega)}\Gamma_{jk}(\omega)e^{i\omega\tau}d\omega\;;\; j,k=1,2,\ldots,m\;;\; j\neq k \qquad (12)$$

In such a case, the component of the non-stationary stochastic vector process are expressed as:

$$f_j^{0}(t)=A_j(t)\;g_j^{0}(t)\;\;;\;\; j=1,2,\ldots,m \qquad (13)$$

where, $g_j^{0}(t)\;;\; j=1,2,...,m$ are the components of a stationary stochastic vector process having mean value equal to zero:

$$\varepsilon\left[g_j^{0}(t)\right]=0\;;\; j=1,2,...,m \qquad (14)$$

and cross-spectral density matrix is given by:

$$S^{0}(\omega,t)=\begin{bmatrix} S_1(\omega) & \sqrt{S_1(\omega)S_2(\omega)}\Gamma_{12}(\omega) & \ldots & \sqrt{S_1(\omega)S_m(\omega)}\Gamma_{1m}(\omega) \\ \sqrt{S_2(\omega)S_1(\omega)}\Gamma_{21}(\omega) & S_2(\omega) & \ldots & \sqrt{S_2(\omega)S_m(\omega)}\Gamma_{2m}(\omega) \\ \vdots & \vdots & \ddots & \vdots \\ \sqrt{S_m(\omega)S_1(\omega)}\Gamma_{m1}(\omega) & \sqrt{S_m(\omega)S_2(\omega)}\Gamma_{m2}(\omega) & \ldots & S_m(\omega,t) \end{bmatrix}_{m\times m} \qquad (15)$$

2.2. FORMULATION FOR m-VARIATE NON-STATIONARY STOCHASTIC PROCESSES

According to the algorithm in Ref. (Deodatis,1996), in order to simulate the 1D-mV non-stationary ground motion vector process $f^0(t)$ the evolutionary cross-spectral density matrix $S_f^0(\omega,t)$ is first decomposed at every time instant t using Cholesky's method into the following product:

$$S_f^0(\omega,t) = H(\omega,t)H^{T*}(\omega,t) \qquad (16)$$

where, $H(\omega,t)$ is a lower triangular matrix and the superscript "T" denotes the transpose of the matrix. $H(\omega,t)$ is written as:

$$H(\omega,t) = \begin{bmatrix} H_{11}(\omega,t) & & & \\ H_{21}(\omega,t) & H_{22}(\omega,t) & & \\ \vdots & \vdots & \ddots & \\ H_{n1}(\omega,t) & H_{n2}(\omega,t) & \cdots & H_{nn}(\omega,t) \end{bmatrix} \qquad (17)$$

The diagonal elements of $H(\omega,t)$ are real and non-negative functions of "ω" satisfying:

$$H_{jj}(\omega,t) = H_{jj}(-\omega,t);\ j=1,2,\ldots,m \quad \forall t \qquad (18)$$

while, the off-diagonal elements are generally complex functions of "ω". Once the cross-spectral density matrix $S_f^0(\omega,t)$ is decomposed according to Eqs 17 and 18, the non-stationary ground motion vector process $f_j^0(t);\ j=1,2,...,m$ can be simulated by the following series as $N\to\infty$:

$$f_j(t) = 2\sum_{r=1}^{m}\sum_{s=1}^{N}\left|H_{jr}(\omega_s,t)\right|\sqrt{\Delta\omega}\cos\left[\omega_s t - \theta_{jr}(\omega_s,t) + \phi_{rs}\right], \quad j=1,2,...,m \qquad (19)$$

where,

$$\theta_{jk}(\omega,t) = \tan^{-1}\left(\frac{\mathrm{Im}\left[H_{jk}(\omega,t)\right]}{\mathrm{Re}\left[H_{jk}(\omega,t)\right]}\right) \qquad (20)$$

in which, Im and Re denote the imaginary and real part of a complex number, respectively. Note that in Eq 16, superscript "0" is omitted to distinguish the vector process $f^0(t)$ from its simulation $f(t)$. The discretization in the frequency domain is done as follows:

$$\omega_s = s\Delta\omega;\ \ s=1,2,...,N;\ \ \Delta\omega = \frac{\omega_c}{N} \qquad (21)$$

In Eq 21, ω_c represents an upper cut-off frequency beyond which the elements of the cross-spectral density matrix may be assumed to be zero at any time instant t. Furthermore, the $\{\phi_{rs}\};\ r=1,2,...,m;\ s=1,2,...,N$ are "m" sequences of "N" independent random phase angles distributed uniformly over the interval $[0,2\pi]$.

3. CASE DESCRIPTION AND MODELING

To investigate of wave passage and incoherency effect on the seismic response of arch dams, DEZ high concrete arch dam was selected as case study. The general overview of this dam is shown in figure 1(a). Total height of the dam is 203m but the height above the concrete plug (the simulated dam) is 194m. Also, the height of the main body (without concrete saddle) is 174m, crest length is 240m, thickness of the dam at the crest is 4.5m and its maximum thickness at the base is 21m [18].

Finite element models of the dam, foundation rock and reservoir were prepared based on as-built drawing, including 792 solid elements for modelling the dam and concrete saddle called as PULVINO (figure 1(b)), 3770 hexagonal solid elements for simulation of mass-less foundation rock and 3660 fluid elements in reservoir domain. In this model mostly hexagonal 8-node elements were used, while prism elements were utilized at portions of the model where geometry was not regular. The reservoir was modelled using hexagonal and prism fluid elements. Utilized EULERIAN fluid elements have three translational degrees of freedom (DOFs) and one pressure DOF in each node, while translational DOFs are active only at nodes that are on the interface with solid elements. Far-end boundary of the foundation is at the distance from the dam, which is about two times the height of the dam body in all directions. It is noteworthy that all contraction and peripheral joints were simulated based on as-built drawings using 3D node-to-node contact elements [18,19] (figure 1(c)).

Mass concrete was supposed as isotropic material where its elasticity and Poisson's ratio in static and dynamic conditions are 40GPa, 46GPa, 0.2 and 0.14 respectively. Mass concrete density is 2400kg/m^3 and its uniaxial tensile strength is 3.4MPa. Isotropic deformation modulus for the foundation rock in the saturated and unsaturated regions is 13GPa and 15GPa, respectively and its Poisson's ratio is assumed to be 0.25. Moreover, reservoir water density was assumed 1000kg/m^3, sound velocity is 1440m/s in water and wave reflection coefficient for the reservoir around boundary is supposed 0.8, conservatively.

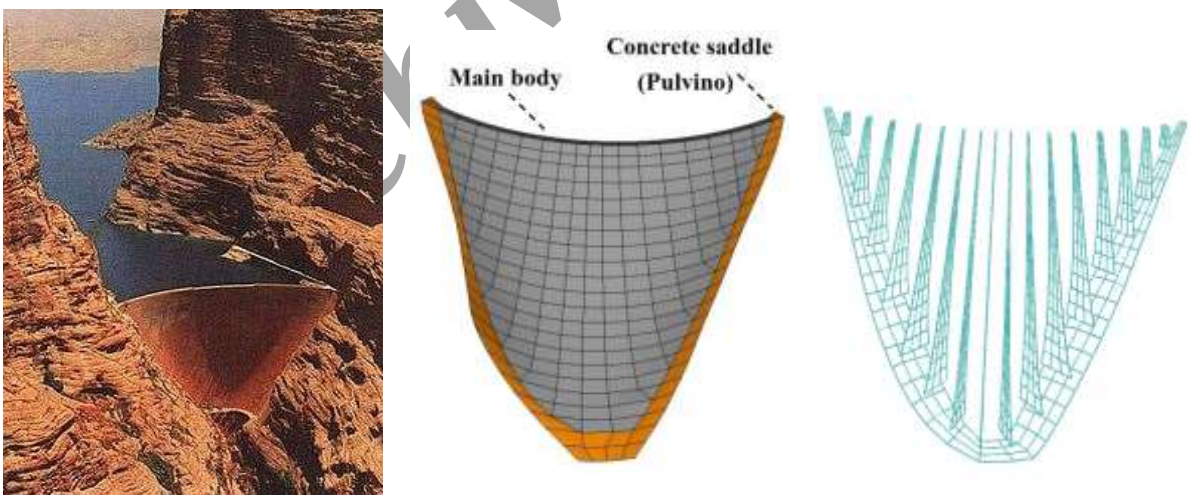

(a) (b) (c)

Figure 1: (a) General overview of DEZ dam, reservoir and surrounding foundation rock, (b) Finite element model of the dam body and its concrete saddle (PULVINO), (c) Contraction and peripheral joints

4. LOADING THE COUPLED SYSTEM

Applied loads on the system are dam body self-weight, hydrostatic pressure in Normal Water Level, thermal load corresponding to summer condition and seismic load. It is worthy to note that thermal load applied on the structure has been extracted from thermal calibration analyses conducted using real data at the dam site taking into account solar radiation on the exposed surfaces of the dam body [19]. In order to comparison of uniform and non-uniform excitation effects on structural responses of the dam body, acceleration response spectrum of the dam site in design base level (DBL) was selected as target spectrum and all artificial ground motions were generated based on horizontal and vertical responses spectrums as shown in figure 2(a). In addition, power spectral of the generated ground motion in uniform excitation is depicted in figure 2(b). Generated ground motions in uniform and non-uniform conditions are applied to the far-end boundaries of the foundation rock and also the reservoir boundaries, simultaneously. In the case of uniform excitation, the applied ground motion in all areas are the same with the first set of non-uniform excitation, while in non-uniform ground motion the system is excited at boundaries using 15 sets of simulated ground motion records compatible with DBL spectrum

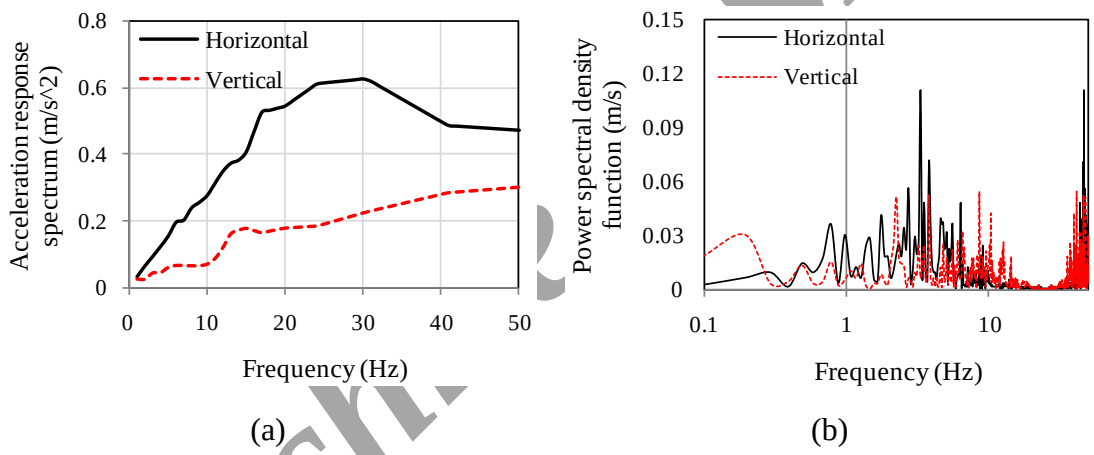

Figure 2: (a) Acceleration response spectrum for the horizontal and vertical components in design base level, (b) Power spectral density function for the horizontal and vertical components in uniform excitation

Based on the presented formulation in previous sections, a computer program was developed for generation of uniform and non-uniform ground motions considering various factors using MATLAB [20]. The program is capable of producing different non-uniform acceleration time-histories considering wave passage and incoherence effects according to the target response spectrum. As mentioned before, the first effect raises by the limited wave propagation velocity, depending on the relative distances of the supporting nodes away from the source. The second effect is due to reflections and refractions of seismic waves through the soil during their propagation that leads to change in amplitude and frequency. In the present paper, effects of wave passage and incoherency on non-uniform excitation of the selected concrete arch dam are investigated. For this purpose four various sets of artificial ground motions were generated in which in the first model only incoherence effect is considered (named as COH); in the second one only wave passage effect is taken into account (named as WPA); in the third one both incoherency and wave passage effects are incorporated (named as CWP) and finally the forth model is excited uniformly (named as UNI). In all cases β-

NEWMARK integration method is utilized to solve the coupled nonlinear problem of the dam-reservoir-foundation system. Moreover, structural damping is taken to be 5% of the critical damping.

5. RESULTS AND DISCUSSION

5.1. DISPLACEMENT AND JOINT BEHAVIOR

Time-history of displacement at the crest point on the central cantilever were extracted in four models and compared with each other as shown in figure 3. Based to this figure, general trend of displacement time-history is similar in all models except COH, which shows lower values. Considering that in the present model positive direction of "y" axis is toward downstream, it can be seen that maximum displacement in UNI and WPA models is occurred at 4.96s toward downstream. In CWP model maximum displacement is at t=2.81s in downstream direction, while in COH model dam intended to vacillate in upstream pertinent area (on the graph) and its maximum value happens at t=3.11s and t=4.96s and is equal to zero. Non-uniform excitation including coherency effect (COH) has minimum displacement, while uniform excitation (UNI) causes maximum displacement. Modelling coherency and wave passage effects simultaneously leads to higher displacement in comparison with MPA and COH. Table 1 summarize extreme values for displacements in upstream and downstream directions for the mid-point, left and right quarter points along the crest. As can be seen, at the mid point the range of the crest movement (Upstream + downstream extreme values) for NUI is largest. In addition, CWP shows the higher fluctuation of the crest mid point in comparison with COH and WPA. As expected, in all models the mid-point shows higher extreme values in comparison with the quarter points.

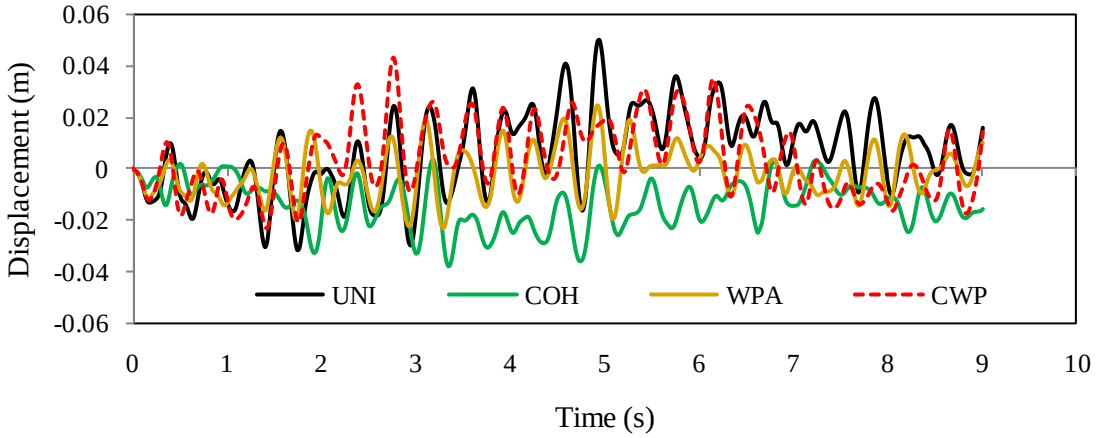

Figure 3: Time-histories of the crest points displacements in the stream direction

Table 1: Extreme values of the displacements in the upstream and downstream directions for the crest points

Models	Mid point		Right quarter point		Left quarter point	
	Upstream (mm)	Downstream (mm)	Upstream (mm)	Downstream (mm)	Upstream (mm)	Downstream (mm)
UNI	51	30	18	18	17	17
COH	0	39	35	0	18	10
WPA	21	20	15	10	6	6
CWP	42	22	25	26	10	18

Figure 4 shows non-concurrent envelopes of joint opening/sliding experienced by upstream contact elements between central blocks. Obviously, coherency (COH) leads to increasing joint opening in upper half of the dam body in comparison with UNI model, while WPA leads to decreasing joint opening. Also modelling incoherency and wave passage effects (CWP) lead to highest value of joint opening among all the considered models. On the other hand, there are no meaningful differences between joint sliding curves for various models, especially in upper half. Anyway, CWP leads to higher joint sliding in lower parts of the body in comparison with the other models. Moreover, WPA model gives higher joint sliding values.

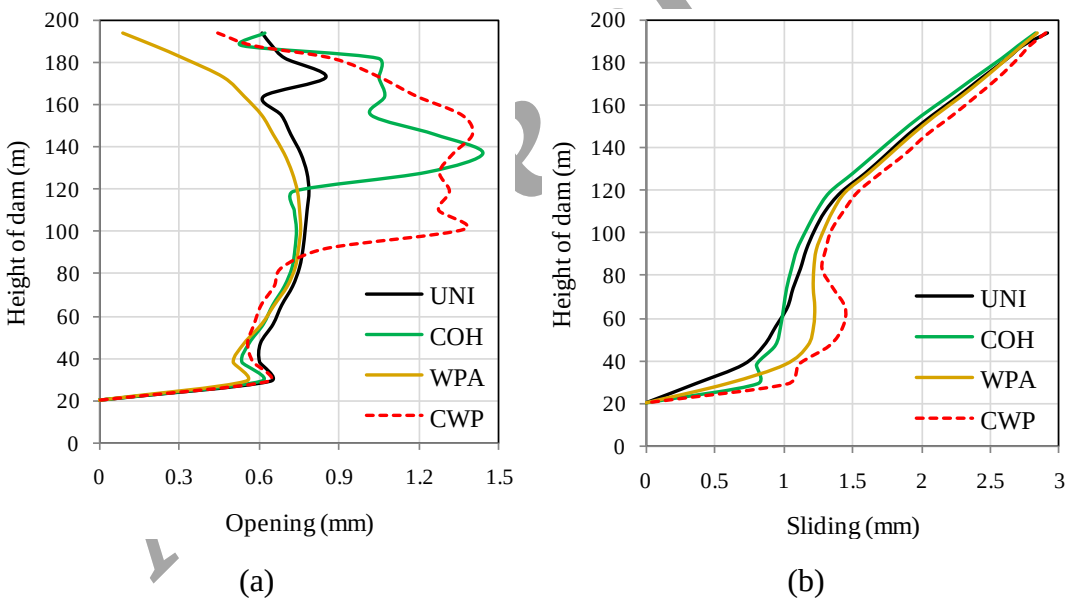

Figure 4: Non-concurrent envelope of (a) Joint opening and (b) Joint sliding; experienced by the upstream contact elements between central blocks

5.2. PRINCIPAL STRESSES

Time-histories of principal stresses at the mid point of the crest are depicted in figure 5. In this figure UNI and CWP are compared with each other. In addition, COH and WPA are compared for considering the significance of the incoherency and wave passage effects. As it is clear, using CWP model leads to higher first principal stress and lower third principal stress at the crest point. On the other hand, COH model leads to

higher extreme values in both principal stresses rather than WPA model. In addition, based on the extracted results for the left and right quarter points, it is concluded that coherency effect overshadow wave passage effect.

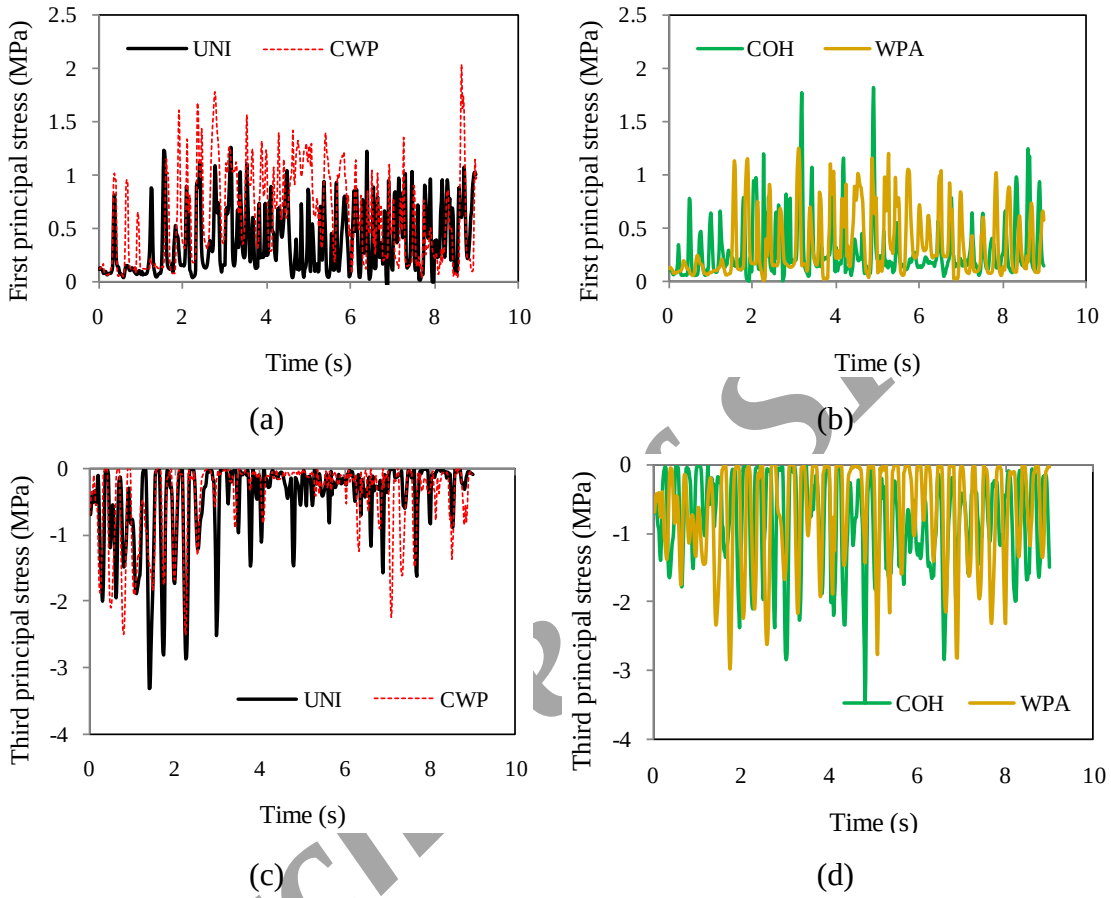

Figure 5: Principal stresses time-histories at the crest mid point; (a) First principal stress for UNI and CWP; (b) First principal stress for COH and WPA; (c) Third principal stress for UNI and CWP; (d) Third principal stress for COH and WPA

Table 2: Extreme values for the first principal stress (MFPS) and third principal stress (MTPS) extracted for the crest points

Models	Mid point		Right quarter point		Left quarter point	
	MFPS (MPa)	MTPS (MPa)	MFPS (MPa)	MTPS (MPa)	MFPS (MPa)	MTPS (MPa)
UNI	1.20	-3.51	1.71	-5.82	1.02	-5.51
COH	1.79	-3.54	1.12	-5.00	0.48	-6.83
WPA	1.21	-3.01	0.70	-5.52	0.35	-5.77
CWP	2.10	-2.47	1.33	-6.03	0.66	-5.53

Figures 6 and 7 show non-concurrent envelopes of principal stresses on upstream and downstream faces of the dam body. As can be seen, in non-uniform excitation MFPS occurs in the lower part of the dam body in vicinity of PULVINO and its value for COH, WPA and CWP models are 7.68MPA, 3.37MPa and 9.69MPa respectively. This value for UNI is 3.85MPa and occurs at the left upper part on the upstream face. It is observed that the wave passage causes decrease of MFPS within the dam body. Also, according to figure 8, it is obvious that incoherency leads to higher stresses in the dam body in comparison with the wave passage phenomenon. Neglecting stress concentration points in the cases with non-uniform excitations, it can be seen that the areas with high stresses shift from left upper parts of the body in uniform excitation to lower parts in non-uniform excitations.

MTPS for NUI occurs at the central part of the upstream face and some areas in vicinity of PULVINO and its value is about -14.3MPa. In CWP model the general pattern is similar to UNI except that MTPS reaches -17.8MPa occurred at the central part on upstream face in vicinity of the crest. For COH model, MTPS is -29.4MPa which occurs in vicinity of PULVINO and for WPA, this value reaches to -12.3MPa at central part of the dam body. It is observed that the model including both incoherency and wave passage has the worst condition based on MTPS among all models. According to these figures it's easy to find that difference between uniform and non-uniform models in MFPS (that can be interpreted as the tensile stress) are more intensive than MTPS (or compressive stress).

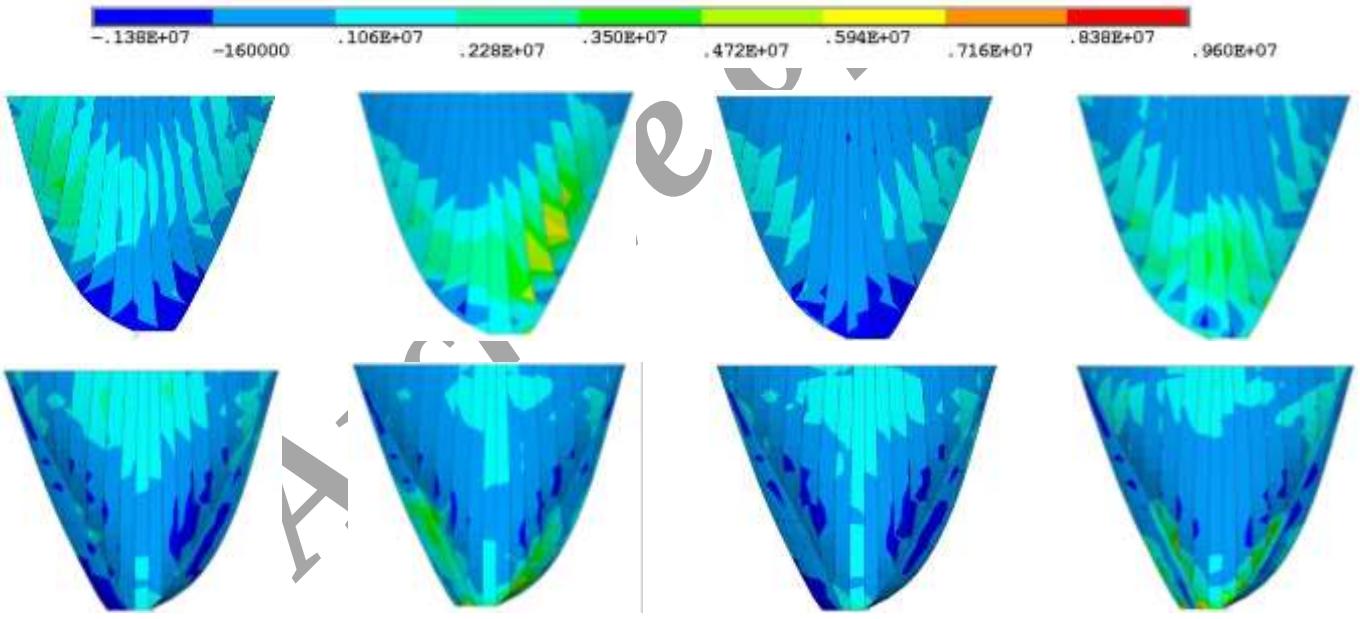

(a) (b) (c) (d)

Figure 6: Non-concurrent envelopes of the first principal stress (MFPS) on the upstream and downstream faces of the dam body (Pa); (a) UNI; (b) COH; (c) WPA; (d) CWP in Pa

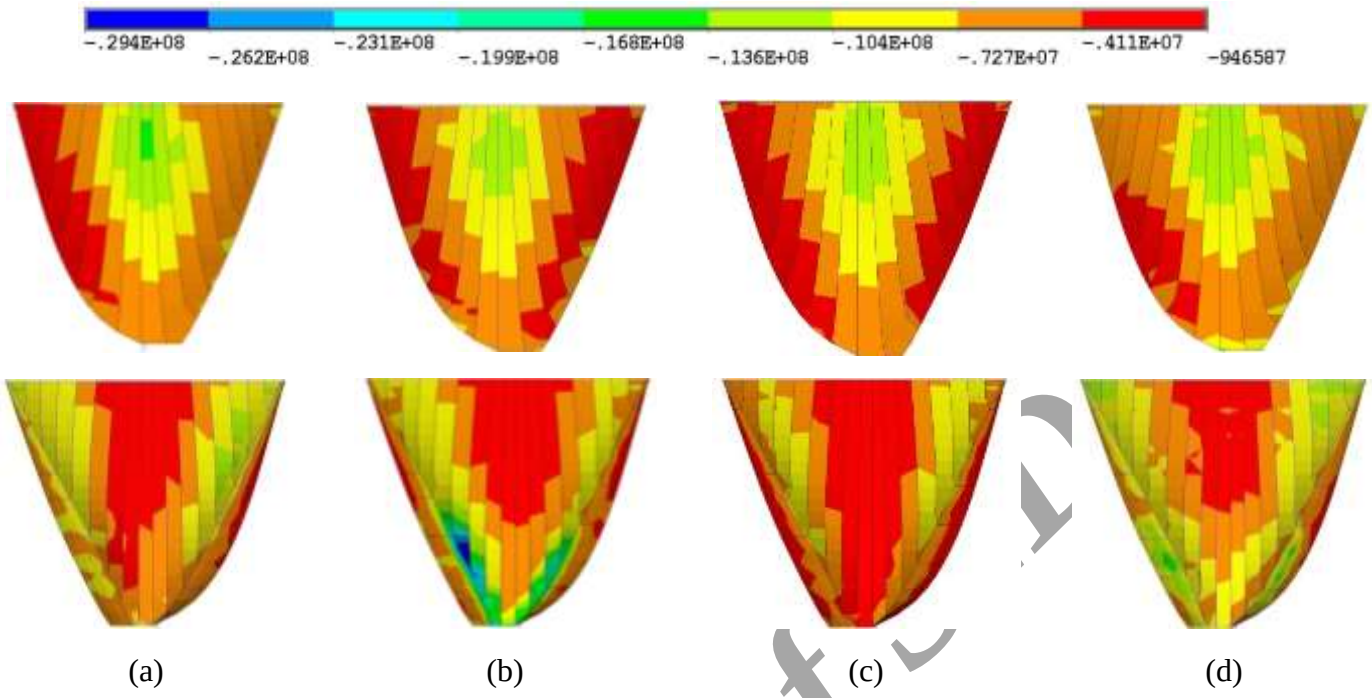

Figure 7: Non-concurrent envelopes of the third principal stress (MTPS) on the upstream and downstream faces of the dam body (Pa); (a) UNI; (b) COH; (c) WPA; (d) CWP in Pa

5.3. HYDRODYNAMIC PRESSURE

Figure 8(a) shows variation of total pressure (hydrostatic + hydrodynamic) at the bottom of the main body (is highlighted in figure 8(b)). As can be seen, uniform excitation leads to higher pressure than non-uniform excitation. The extreme values for the hydrodynamic pressures experienced by the considered point are 147KPa for UNI, 93KPa for COH, 99KPa for WPA and 83KPa for CWP model. In addition, maximum pressure experienced by the bottom point for UNI, COH, WPA and CWP models are 1.853MPa, 1.799MPa, 1.805MPa and 1.783MPa respectively. So COH model leads to more reduction in hydrodynamic pressure in comparison with WPA model and also modelling both incoherency and wave passage leads to minimum hydrodynamic pressure among all the non-uniform models.

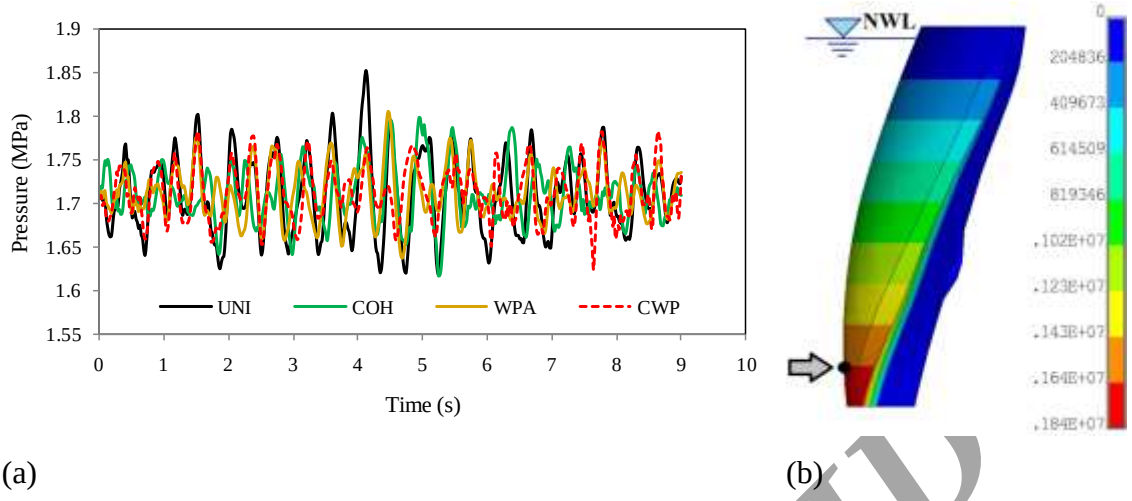

(a) (b)

Figure 10: (a) Variation of water pressure at the specified point on the upstream face; (b) Hydrostatic pressure on the upstream face of the dam body in normal water level condition and location of the reference point

6. CONCLUSION

In the present paper, effects of non-uniform excitation due to spatially variation earthquake ground motions (SVEGM) on nonlinear responses of a high concrete arch dam were studied. Generally, SVEGM models include incoherency, wave-passage and site response effects. The incoherence effect was considered by using Harichandran and Vanmarcke coherency model and the effect of wave passage was modeled choosing a limited wave propagation velocity. Four cases were considered which are: uniform excitation (UNI), incoherency (COH), wave passage (WPA) and finally, incoherency and wave passage simultaneously (CWP). Monte-Carlo simulation approach was used in generation of SVEGM. DEZ dam located in south west of Iran was chosen for case study and finite element model of the dam-reservoir-foundation rock was provided in which all contraction joints and also, peripheral joint between the main dam and its concrete saddle were modelled as shown in as-built drawings.

It was concluded that uniform excitation leads to higher crest movement in comparison with the cases of non-uniform input. In addition, considering both incoherency and wave passage (CWP) leads to higher displacement at the crest in comparison with the two other non-uniform cases (COH and WPA). UNI is more similar to WPA in the first principal stress envelopes and coherency effect overshadow wave passage effect for stress responses.

Maximum joint sliding for the considered cases are almost the same along the crown cantilever but CWP leads to little more joint sliding. COH and CWP models lead to higher joint opening than UNI model and WPA leads to lower joint opening along crown cantilever. In addition, it was found that that results obtained from WPA is close to the corresponding ones in UNI. It was observed that minimum third principal stress (MTPS) in non-uniform excitation is less than uniform excitation; also wave passage effect leads to reduction of maximum first principal stress (MFPS) on upstream and downstream faces of the dam body. Also it was observed that incoherence effects create higher stresses in the dam body and intensify wave passage effect. Differences between uniform and non-uniform inputs for MFPS (as tensile stress) are more intensive than MTPS (as compressive stress). Also, it was concluded that differences between uniform and non-uniform excitations in MFPS is more than MTPS.

Generally, non-uniform excitation generates higher tensile and compressive stresses in dam body. On the other hand, COH model leads to more reduction in hydrodynamic pressure than WPA model and also modelling both incoherency and wave passage effects leads to minimum hydrodynamic pressure among all the models excited non-uniformly. Therefore, the SVEGM has important effects on the seismic response of the dam-reservoir-foundation coupled system and to be more realistic in calculating the dam response, SVEGM should be incorporated in dam analysis and design.

REFERENCES

[1] Harichandran, R.S. and Wang, W.; " Response of simple beam to spatially varying earthquake excitation "; J Eng Div, ASCE, NO.114(9) (1988) 1526–41.
[2] Zerva, A., " Effect of spatial variability and propagation of seismic ground motions on the response of multiply supported structures"; Journal of Probabilistic Engineering Mechanics, N0.6(3-4) (1991) 212–21.
[3] Zerva, A.; " Response of multi-span beams to spatially incoherent seismic ground motions"; Earthquake Engineering and Structural Dynamics, NO.19(6) (1990)819–32.
[4] Zerva, A.; " Seismic loads predicted by spatial variability models"; Struct Safety , 11(3–4) (1992)227–43.
[5] Zerva, A.; " On the spatial vibration of seismic ground motions and its effects on lifelines"; Eng Struct,NO.16(1) (1994)534–46.
[6] Bayraktara, A., Hancera, E., Dumanoglu, AA.; " Comparison of stochastic and deterministic dynamic responses of gravity dam–reservoir systems using fluid finite elements, " Finite Elements in Analysis and Design, NO.41(2005)1365–1376.
[7] Maeso, O., Aznarez, J.J. and Dominguez, J.; "Effects of space distribution of excitation on seismic response of arch dams"; Journal of Engineering Mechanics, ASCE, NO.128(2002)759-768.
[8] Chen, M.T. and Harichandran, R.S.; "Response of an earth dam to spatially varying earthquake ground motion"; Journal of Engineering Mechanics, ASCE, NO.127(2001) 932-939.
[9] Mirzabozorg, H., Varmazyari, M. and Ghaemian, M.; "Dam- reservoir-massed foundation system and travelling wave along reservoir bottom"; Soil Dynamics and Earthquake Engineering, NO.30(2010)746–756.
[10] Mirzabozorg, H., Kianoush, R. and Varmazyari, M.; "Nonlinear Behavior of Concrete Gravity Dams and Effect of Input Spatially Variation";Structural Engineering and Mechanics, No. 3(35) (2010) 365-379.
[11] Bayraktar, A. and Dummsnoglu, A.A.;"The effect of synchronous ground motion on hydrodynamic pressures"; Computer and structures, NO.68 (1998) 271-282.
[12] Bayraktar, A. and Dummsnoglu, A.A. and Calayir Y.; "Asynchronous dynamic analysis of dam-reservoir-foundation systems by the Lagrangian approach"; Computer and structures, NO.58(1996) 925-935.
[13] Alves, S.W. and Hall, J.F.; "Generations of spatially nonuniform ground motion for nonlinear analysis of a concrete arch dam" ;Earthquake Engineering and Structural Dynamics, NO.35(2006) 1339-1357.
[14] Alves, S.W. and Hall, J.F.; "System identification of a concrete arch dam and calibration of its finite element model"; Earthquake Engineering and Structural Dynamics, NO.35(2006) 1321-1337.
[15] Chopra, A. and Wang, J.; "earthquake response of arch dams to spatially varying ground motion"; earthquake engineering and structural dynamics, NO.39 (8) (2010)887-906.
[16] Shinozuka, M. and Deodatis, G.; "Stochastic process models of earthquake ground motion"; Journal of Probabilistic Engineering Mechanics, NO.3(3) (1988)114–23.
[17] Cacciola, P. and Deodatis, G.; "A method for generating fully non-stationary and spectrum-compatible ground motion vector processes"; Soil Dynamics and Earthquake Engineering ,NO.31(3) (2010) 351-360.
[18] Hariri Ardebili, M.A., Mirzabozorg, M., Ghaemian, M., Akhavan, A. and Amini, A.; "Calibration of 3D FE model of DEZ high arch dam in thermal and static conditions using instruments and site observation";6th International conference on dam engineering. Lisbon, Portugal, (2011)121-135.
[19] Mirzabozorg, H., Hariri Ardebili, M.A. and Amirpour, A.; "Material and Joint Nonlinearity Effects on Seismic Performance Evaluation of High Concrete Arch Dams"; 9th International Congress on Advances in Civil Engineering, Trabzon, Performance Evaluation, Turkey, Sep, 2010.
[20] MATLAB R2007a. (2007), MathWorks, Inc.